IEICE TRANS. COMMUN., VOL.E90–B, NO.9 SEPTEMBER 2007

PAPER Special Section on 2006 International Symposium on Antennas and Propagation

A Method of Measuring Gain in Liquids Based on the Friis Transmission Formula in the Near-Field Region

Nozomu ISHII[†,††a)], *Member*, Takuhei AKAGAWA[†††*], *Student Member*, Ken-ichi SATO[††††], *Nonmember*, Lira HAMADA[††], *and* Soichi WATANABE[††], *Members*

SUMMARY In the 300 MHz to 3 GHz range, probes used to measure specific absorption rate (SAR) of mobile communication devices are usually calibrated using a rectangular waveguide filled with tissue-equivalent liquid. Above 3 GHz, however, this conventional calibration can be inaccurate because the diameter of the probe is comparable to the cross-sectional dimension of the waveguide. Therefore, an alternative method of SAR probe calibration based on another principle was needed and has been developed by the authors. In the proposed calibration method, the gain of the reference antenna in the liquid is first evaluated using the two-antenna method based on the Friis transmission formula in the conducting medium. Then the electric field intensity radiated by the reference antenna is related to the output voltage of the SAR probe at a given point in the liquid. However, the fields are significantly reduced in the liquid, and the gain is impossible to calibrate in the far-field region. To overcome this difficulty, the Friis transmission formula in the conducting medium must be extended to the near-field region. Here, we report results of simulations and experiments on estimated gain based on the extended Friis transmission formula, which holds in the near-field region, and test the validity of the new formula.

key words: *Friis transmission formula, SAR probe calibration, conducting medium, Fresnel approximation, far-field gain*

1. Introduction

A new calibration method for specific absorption rate (SAR) probes was needed to evaluate SAR values of mobile communication devices operating in the range above 3 GHz. The conventional calibration method, which uses a waveguide filled with tissue-equivalent liquid [2], [3] is widely used for devices operating in the 300 MHz to 3 GHz range [2]. However, the strong effect of the probe diameter affects calibration at higher frequencies, especially when the diameter is comparable to the cross-sectional dimension of the waveguide above 3 GHz. We developed an alternative calibration method [4]–[6].

In our proposed calibration, the gain of the reference antenna in the liquid [7] is evaluated using the two-antenna method based on the Friis transmission formula in the conducting medium [8]. The SAR probe can be calibrated by relating the electric field intensity radiated by the reference antenna to the output voltage of the probe at a point in the liquid [2], [9]. S parameters between two identical reference antennas are measured to evaluate the gain of the reference antenna. In other words, two identical antennas are connected to ports 1 and 2 of the vector network analyzer, and then the magnitude and phase of S_{21} between the two ports are measured as a function of the distance between the two antennas. The data measured is fit to curves derived from the Friis transmission formula in the far-field region, and then the gain of the reference antenna, the attenuation, and the phase constants of the medium, α, β, can be estimated [11].

However, the decay in the liquid is so enormous that the measurement of S_{21} is difficult in the far-field region [6]. For example, the attenuation constant in the liquid is about 464 dB/m at 2.45 GHz. Above 3 GHz, the decay is even greater, so that measurable range for S_{21} is much shorter than the one expected from the scaling rule of the wavelength for the frequency. At the time of writing, we have studied the following solutions.

1. Inserting amplifiers between the reference antenna and port 1 of the vector network analyzer to increase the input power to the measurement system, P_{in}.
2. Measuring the magnitude of S_{21} as a function of the distance between the antennas using a spectrum analyzer instead of the vector network analyzer to ensure a wide dynamic range of the measurement system. Since the phase of S_{21} cannot be measured using the spectrum analyzer, the permittivity of the liquid must be measured by the contact probe or another method.
3. Fitting measured S_{21} to the curves based on the Friis transmission formula, which holds in the near-field region of the antenna in the liquid, to avoid curve fitting in the far-field region.

This paper reports results for item 3). The Friis transmission formula in the near-field region of the antennas in free space was studied to estimate the gain of relatively large-scale aperture antennas; the gain is represented by a function of the distance from the antenna and determined by its convergent value [14], [15]. However, the authors know of no published description of the behavior of the fields or of the Friis transmission formula in the near-field region of

Manuscript received December 26, 2006.
Manuscript revised April 10, 2007.

[†]The author is with the Faculty of Engineering, Niigata University, Niigata-shi, 950-2181 Japan.
[††]The authors are with the National Institute of Information and Communications Technology, Koganei-shi, 184-8795 Japan.
[†††]The author was with the Graduate School of Science and Technology, Niigata University, Niigata-shi, 950-2181 Japan.
[††††]The author is with the NTT Advanced Technology, Musashino-shi, 182-0012 Japan.
*Presently, with the Toyo Corporation.
a) E-mail: nishii@eng.niigata-u.ac.jp

DOI: 10.1093/ietcom/e90–b.9.2401

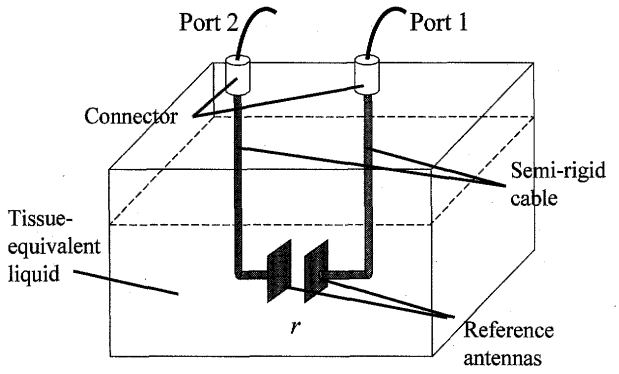

Fig. 1 Measurement set-up for gain of antenna in liquid.

the antenna in the conducting medium.

In this paper, the Friis transmission formula, which holds in the near-field region of the antenna in the conducting medium, is proposed by abstracting features from both the Friis transmission formula in the near-field region of the antenna in free space [15] and the Fresnel approximations in free space [16]. In order that a physical aspect of the new formula could be discussed, the distance dependence of the electric field in the near-field region was examined for a dipole antenna and was extended for an arbitrary antenna. In addition, the target functions for curve fitting are rewritten on the basis of the extended Friis transmission formula in the near-field region. Finally, new curve fitting for simulated and measured data is used to confirm the validity of this new formula. The effect of enhancing the dynamic range of the system is also discussed.

2. Friis Transmission Formula in the Far-Field Region

Two polarization-matched antennas are aligned for maximum directional radiation in the liquid, as shown Fig. 1. If the distance between the two antennas, r, is sufficiently large, the ratio of transmitted power, P_1, to received power, P_2 (the Friis transmission formula in the far-field region) can be expressed as [8]

$$|S_{21}|^2 = \frac{P_2}{P_1} = (1-|S_{11}|^2)(1-|S_{22}|^2)\frac{|G_1||G_2|e^{-2\alpha r}}{4\beta^2 r^2}, \quad (1)$$

where S_{ij} are S parameters between the ports of two antennas, $|G_i|$ are the magnitude of the gain of antenna i, and α and β denote the attenuation and phase constants in the liquid, respectively. The subscript i indicates the transmitting or receiving antennas for $i = 1$ or 2. (1) can be rewritten in dB form as

$$|S_{21}|_{\mathrm{dB}} = A - 20\log_{10} r - 8.686\alpha r. \quad (2)$$

$|S_{21}|_{\mathrm{dB}}$ can be measured as a function of distance r and a constant A and the attenuation constant α can be determined by the curve fitting for $|S_{21}|_{\mathrm{dB}}$ based on (2). The sum of the gains in dB form can be expressed as

$$(G_1)_{\mathrm{dB}} + (G_2)_{\mathrm{dB}} = A + 20\log_{10}(2\beta) - (M_1)_{\mathrm{dB}} - (M_2)_{\mathrm{dB}}, \quad (3)$$

where $(M_i)_{\mathrm{dB}} = 10\log_{10}(1-|S_{ii}|^2)$ is the dB form of the mismatch or reflection efficiency of antenna i. If the two antennas are identical, their gains are equal. Then, (3) can be reduced as

$$G_{\mathrm{dB}} = \frac{1}{2}[A + 20\log_{10}(2\beta) - (M_1)_{\mathrm{dB}} - (M_2)_{\mathrm{dB}}]. \quad (4)$$

In the conventional two-antenna method, constant A or gain G_{dB} can be determined at distance r in accordance with (2) or (4). Our method is more accurate than the conventional one because A is determined by curve fitting. The phase constant β in the liquid is required to evaluate the gain in accordance with (4) and it can be determined by the contact probe method. However, phase constant β is determined by measuring $\angle S_{21}$ as a function of distance r in our method. When an electromagnetic wave travels in the liquid, phase shift is expressed by a linear function of distance r as follows:

$$\angle S_{21} = -\beta r + B, \quad (5)$$

where $B = (\angle G_1 + \angle G_2)/2$ is an arithmetic mean value of fictitious phases of the gains of two antennas. $\angle S_{21}$ can be measured as a function of distance r and phase constant β can be determined by the curve fitting for $\angle S_{21}$ based on (5). This curve fitting can be carried out using the linear least-square method.

The following equation can be obtained by combining (1) and (5):

$$S_{21}^2 = (1-|S_{11}|^2)(1-|S_{22}|^2)\frac{G_1 G_2 e^{-2\gamma r}}{4\beta^2 r^2}, \quad (6)$$

where $\gamma = \alpha + j\beta$ is the propagation constant in the liquid and $G_i = |G_i|\exp(j\angle G_i)$ can be viewed as a complex gain of the antenna i. Thus, the distance dependence of S_{21} between antennas can be expressed as

$$f(r) = \frac{e^{-\gamma r}}{r}. \quad (7)$$

The above expression is identical to the distance dependence of the electric field in the far-field region of a point source located at the origin. However, it cannot entirely explain the behavior of S_{21} in the near-field region of the antennas because the fields in that region depend on the dimension of the antenna.

Because the attenuation and phase constants, α and β, can be determined in the process of obtaining the gain, we can also specify the electrical property of the liquid as follows:

$$\varepsilon_r = \frac{\beta^2 - \alpha^2}{\omega^2 \mu_0 \varepsilon_0}, \quad (8)$$

$$\sigma = \frac{2\alpha\beta}{\omega\mu_0}, \quad (9)$$

where $\omega = 2\pi f$, f is the operating frequency and μ_0 and ε_0 are the permeability and permittivity in free space. Thus, we can estimate the dielectric constant, ε_r, and the conductivity, σ, of the liquid as well as the gain of the antenna in the liquid.

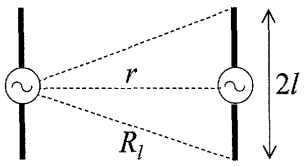

Fig. 2 Distance between middle point of one dipole antenna and end of other dipole antenna.

3. An Extension of the Friis Transmission Formula in the Conducting Medium

3.1 Fresnel Approximation in the Conducting Medium

To review the physical meaning of the near-field effect, let us consider two dipole antennas with a length of $2l$, which face each other. If the distance between them is denoted as r, the distance between the middle point of the dipole antenna and the end of the other antenna can be expressed as $R_l = \sqrt{r^2 + l^2}$, as shown in Fig. 2. If two antennas are closer, but $l/r \ll 1$, R_l can be approximated as

$$R_l = r\sqrt{1 + \left(\frac{l}{r}\right)^2} \approx r + \frac{l^2}{2}\frac{1}{r}. \tag{10}$$

It can be found that the distance between any points on two antennas, denoted as R, may include the contribution of $1/r$ as well as r. The term of $1/r$ dominantly contributes to R or the behavior of the fields because r is close to zero.

To derive an extension of the Friis transmission formula in the conducting medium (1), let us consider that the current distribution of the transmitting antenna is expressed as $\mathbf{J}(\mathbf{r})$. Therefore, the electric field at the center of the receiving antenna $\mathbf{E}(\mathbf{r})$ is given by [17]

$$\mathbf{E}(\mathbf{r}) = -j\omega\mu\left[\bar{\mathbf{I}} - \frac{1}{\gamma^2}\nabla\nabla\right] \cdot \iiint_v \mathbf{J}(\mathbf{r}')\frac{e^{-\gamma|\mathbf{r}-\mathbf{r}'|}}{4\pi|\mathbf{r}-\mathbf{r}'|}dv', \tag{11}$$

where $\mathbf{r}$ and $\mathbf{r}'$ denote the position vectors at the center of the receiving antenna and at any point on the transmitting antenna, respectively, and $\bar{\mathbf{I}}$ denotes the unit dyad. For the Fresnel approximation, the distance between two points can be approximated as

$$R = |\mathbf{r} - \mathbf{r}'| \approx r - \hat{\mathbf{r}} \cdot \mathbf{r}' + \frac{a(\mathbf{r}')}{r}, \tag{12}$$

where $r = |\mathbf{r}|$, $\hat{\mathbf{r}} = \mathbf{r}/r$, $r' = |\mathbf{r}'|$, and $a(\mathbf{r}') = \{r'^2 - (\hat{\mathbf{r}} \cdot \mathbf{r}')^2\}/2$. If a constant, b, can be selected as

$$\iiint_v \mathbf{J}(\mathbf{r}')e^{\gamma\hat{\mathbf{r}}\cdot\mathbf{r}' - a(\mathbf{r}')/r}dv' = e^{-b/r}\iiint_v \mathbf{J}(\mathbf{r}')e^{\gamma\hat{\mathbf{r}}\cdot\mathbf{r}'}dv', \tag{13}$$

then, (11) can be approximated as

$$\mathbf{E}^{\text{near}}(\mathbf{r}) = -j\omega\mu\left[\bar{\mathbf{I}} - \frac{1}{\gamma^2}\nabla\nabla\right] \cdot \frac{e^{-\gamma r - b/r}}{4\pi r}\iiint_v \mathbf{J}(\mathbf{r}')e^{\gamma\hat{\mathbf{r}}\cdot\mathbf{r}'}dv'. \tag{14}$$

This expression includes the propagation factor, $e^{-\gamma r}$, and the far-field term of the spatial spreading factor, $1/r$, as is the case for the far-field approximation. Obviously, if $b = 0$, (14) reduces to the expression for the far-field region. It is noted that electric field $\mathbf{E}^{near}(\mathbf{r})$ includes factor $e^{-b/r}$, which determines the behavior of the the near field of the antenna. If $\mathrm{Re}(b) > 0$, the larger magnitude of the electric field can be observed as distance r approaches zero. This contribution diminishes in the far-field region. Therefore, the distance dependence of S_{21} between two antennas should be extracted and approximated as

$$f(r) = \frac{e^{-\gamma r}}{r}e^{-b/r}. \tag{15}$$

Except for the attenuation due to the surrounding medium, this asymptotic expansion is similar to the Friis transmission formula in the near-field region of the lossless medium, especially free space [15]. In free space, the phase of S_{21} in the near-field region can be affected by the contribution of the distance dependence of $1/r$ as well as r [16]. In the conducting medium, both phase shift and exponential decay with a distance dependence of $1/r$ are included in the fields of the near-field region.

3.2 Friis Transmission Formula in the Near-Field Region

As expected from (15), S_{21}^{near} measured in the near-field region can be related to S_{21} in the far-field region as follows:

$$\begin{aligned}(S_{21}^{\text{near}})^2 &= S_{21}^2 e^{-2b/r} \\ &= (1 - |S_{11}|^2)(1 - |S_{22}|^2)\frac{G_1 G_2 e^{-2\gamma r}}{4\beta^2 r^2}e^{-2b/r}\end{aligned} \tag{16}$$

Thus, the distance dependence of $|S_{21}|_{\text{dB}}$ in the near-field region can be replaced as

$$|S_{21}^{\text{near}}|_{\text{dB}} = A - 20\log_{10} r - 8.686\alpha r + \frac{A_1}{r}, \tag{17}$$

where A_1 is a constant. $|S_{21}|_{\text{dB}}$ can be measured as a function of distance r and A, α, and A_1 can be determined by curve fitting for $|S_{21}|_{\text{dB}}$ based on (17). The sum of gains in dB form of two antennas is given by (3) as before. Similarly, the distance dependence of $\angle S_{21}$ in the near-field region can be replaced as

$$\angle S_{21}^{\text{near}} = -\beta r + B + \frac{B_1}{r}, \tag{18}$$

where B_1 is a constant. $\angle S_{21}$ can be measured as a function of distance r and β, B and B_1 can be determined by curve fitting for $\angle S_{21}$ based on (18).

The above curve fittings in the near-field region can be carried out using the least square method.

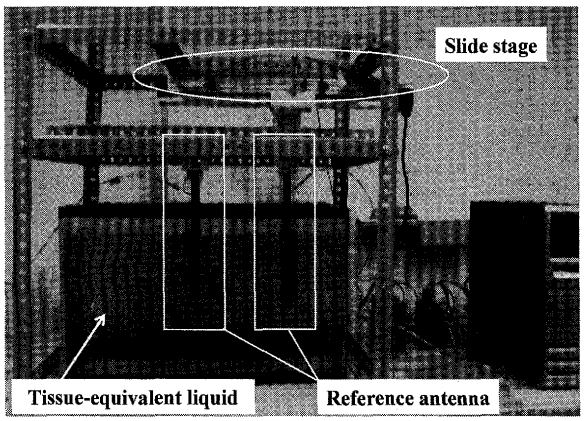

Fig. 3 Measurement setup. Two reference antennas in tissue-equivalent liquid are connected to slide stage so as to control their separation.

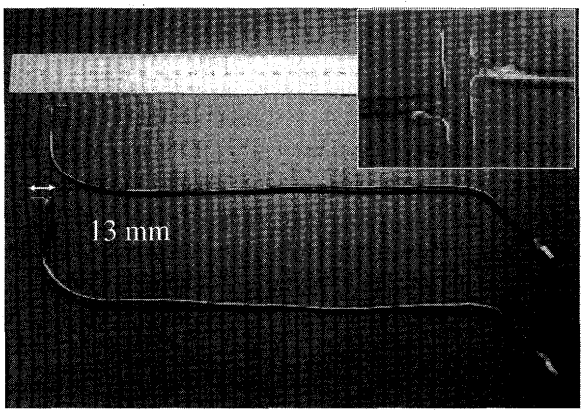

Fig. 4 Offset-fed dipole antennas and semi-rigid cables.

4. Fitting Results

4.1 Far-Field Fitting for Measured Data

The conducting medium assumed in this paper is the tissue-equivalent liquid for the SAR estimation [2], [3] at 2.45 GHz. The liquid should ideally have a permittivity of 39.2 and conductivity of 1.80 S/m according to the IEC document [2]. In practice, it has a permittivity of 39.7 and conductivity of 1.84 S/m at 22°C, which can be measured using the contact probe method.

Figure 3 shows our measurement setup. A rectangular tank has a width of 600 mm, a depth of 300 mm and a height of 350 mm and is filled with 50 l of the tissue-equivalent liquid [3]. The receiving antenna is fixed, while the transmitting antenna is moved with a stage operated by its controller. To avoid connection through the liquid, the antennas are located at the ends of semi-rigid cables, as shown in Fig. 4. No balun is used because the unbalanced current would be rapidly degraded in the liquid [11]. In the measurement, S_{21} can be measured in the range from $r = 0$ mm to 150 mm in increments of 0.5 mm, so S_{11} and S_{22} are measured at $r = 150$ mm. The values of the return loss of the offset-fed dipole antenna are −14.7 dB and −13.9 dB.

Next, we discuss the measurable range and level by

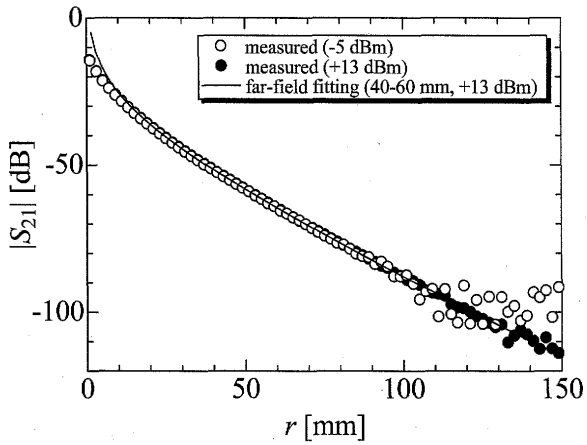

Fig. 5 Measured $|S_{21}|_{\mathrm{dB}}$ and its curve fitting based on Friis transmission formula in far-field region.

measuring $|S_{21}|$ between two dipole antennas that face each other. The length of the dipole antenna is 13 mm and more than half of its effective length is submerged in the liquid to realize the matching condition. Figure 5 shows the measured $|S_{21}|$ as a function of the distance, r. The output power level of the network analyzers (Agilent N5230A) were set to −5 dBm or +13 dBm. The attenuation is mainly caused by conducting loss in the liquid and by insertion loss in the RF cables. The influence from rods that support the semi-rigid cables is measured as the distance between the antenna and the rod is varied. This results in curvature of the semi-rigid cable, as shown in Fig. 4. At −5 dBm input, the measured data hardly fluctuate at $r = 80$ mm, but fluctuate greatly at $r = 100$ mm, as shown in Fig. 5. This is because the noise level of the measurement system is smaller than the signal level at $r = 80$ mm and is larger at $r = 100$ mm. For reference, the values of $|S_{21}|$ are about −76.0 dB and −86.8 dB at $r = 80$ mm and 100 mm, respectively. At +13 dBm, the dynamic range can be expanded so that the data can be measured at the level of about −105 dB, that is, until $r = 130$ mm.

Figure 6 shows the estimated gain of the dipole antenna in the liquid determined by the curve fitting for the measured S_{21} based on the Friis transmission formula in the far-field region [6], which we refer to as far-field fitting. The horizontal axis in this graph, r_c, denotes the center of the fitting range $[r_c - \Delta r, r_c + \Delta r]$, where Δr denotes the width of the fitting range. For simplicity, r_c is written as r in this figure. At input of −5 dBm, the estimated gain with no fluctuation can be obtained up to $r = 65$ mm for $\Delta r = 20$ mm and 50 mm, and then its noise increases as r increases. The gain cannot be estimated when $r \geq 70$ mm. Therefore, the gain should be estimated using measured data up to $r = 70$ mm. Moreover, as shown in Fig. 6, the estimated gain only converges momentarily, after which it starts fluctuating a lot. At input of +13 dBm, the estimated gain with no fluctuation can be obtained up to $r = 100$ mm. Clearly, the measurable range can widen as the dynamic range is extended. Also, it can be seen that the gain tends to be greatly affected by the fluctuation of the system so that the enhancement of the dynamic

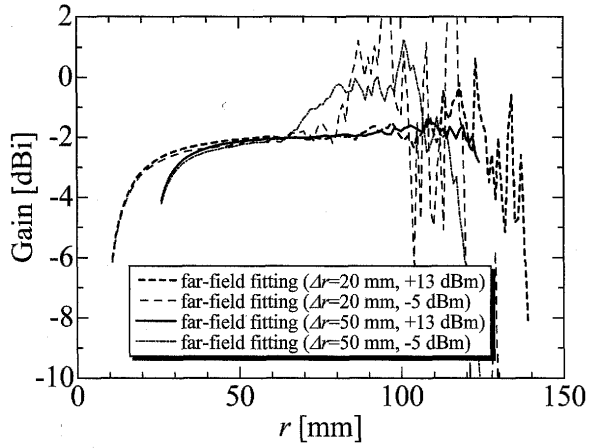

Fig. 6 Estimated gain by curve fitting for measured S_{21} based on Friis transmission formula in far-field region.

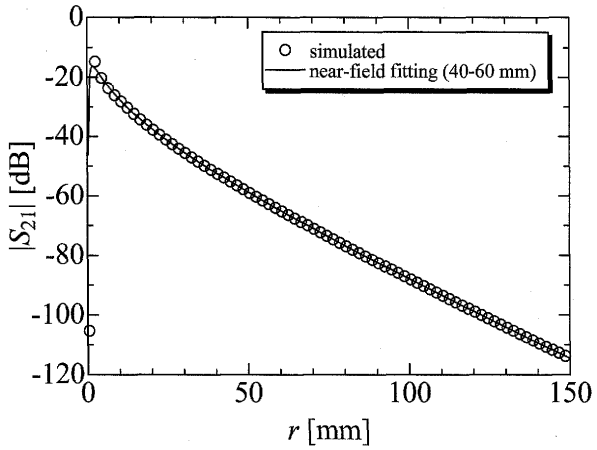

Fig. 7 Simulated $|S_{21}|$ and its curve fitting based on extended Friis transmission formula in near-field region.

range is essential to stable gain measurement in the liquid. However, as the estimated gain slowly converges with the far-field gain in the range as shown in Fig. 6. Based on the results of the far-field fitting for [40 mm, 60 mm], the permittivity and conductivity of the liquid are estimated to be 38.45, and 1.82 S/m and the far-field gain is estimated to be −2.08 dBi. As described above, a strong solution is required to overcome the slow convergence of the estimated gain.

4.2 Validity Check of New Formula Using Simulated Data

Measurement of S parameters between two offset-fed dipole antennas that are facing each other in the liquid can be simulated by the methods of moment for the thin-wire structure in the conducting medium coded by Richmond [4], [18]. The code can output the performance of the antenna, the characteristics of the wave propagation and the coupling effect between antennas in the liquid. It can also simulate them very quickly, in contrast with the large-scaled numerical computations, for example, FDTD. The short-time computation is attractive in simulating the gain calibration, which is required to plot the field at many points. Of course, this code simulates S_{21} with no noise so that we can determine the minimum distance r_c that the curve fitting is valid in the far-field region.

Next, we present an example of the curve fitting for the simulated data at 2.45 GHz based on the Friis transmission formula in the near-field region, which we refer to as near-field fitting. The dipole antenna has a length of l = 13 mm and is fed by the internally dividing point at a ratio of 5:8. The wire is assumed to have the diameter of 1 mm and a conductivity of 5.8×10^7 S/m. In the fitting range [40 mm, 60 mm], the permittivity and conductivity in the liquid is estimated to be 39.15 and 1.80 S/m, which are almost equal to their preset values. The estimated gain is −1.04 dBi, which is nearly equal to the gain obtained by the code developed by Richmond, −1.13 dBi. Another estimated gain obtained by the far-field fitting is −1.40 dBi, which is slightly lower than the true value of the gain.

Figure 7 shows the simulated $|S_{21}|$ and corresponding

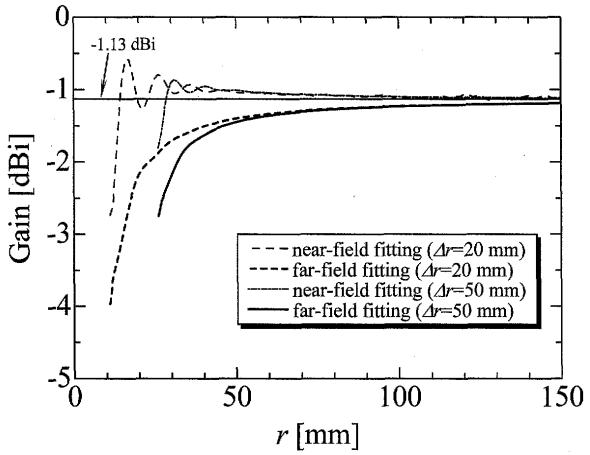

Fig. 8 Estimated gain of center-fed dipole antenna by curve fitting for simulated S_{21} based on extended Friis transmission formula in near-field region.

near-field fitting curve as a function of r. The curve fitting is carried out in the range of [40 mm, 60 mm]. Both curves in Fig. 7 are in good agreement with each other except in close proximity to the antenna. Figure 8 shows the estimated gain defined by (4) and (17), which we refer to as near-field gain, of the dipole antenna in the liquid determined by the near-field fitting for the simulated S_{21}. Figure 8 also shows another estimated gain determined by the far-field fitting, which we refer to as far-field gain. The near-field gain estimated by using the data near the antenna converges with the far-field gain. This suggests that the gain can be estimated by fitting the data measured near the transmitting antenna to the Friis transmission formula in the near-field region. The estimated gains are in good agreement with the true gain simulated by the methods of moment. It is found that a wider range is required for the far-field gain to converge as shown in Fig. 8. Although the far-field distance of the dipole antenna is given by $R_{ff} = 2l^2/\lambda_e = 2(13)^2/9.8 = 34.5$ mm, the far-field gain at r = 70 mm is somewhat suspect on the basis that the data simulated should be satisfied with our empirical far-field condition of $r > 5\lambda_e$, where $\lambda_e = 2\pi/\beta$ is

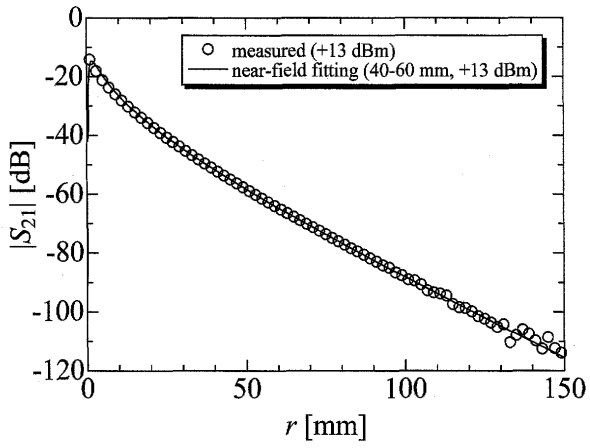

Fig. 9 Measured $|S_{21}|$ and its curve fitting based on extended Friis transmission formula in near-field region.

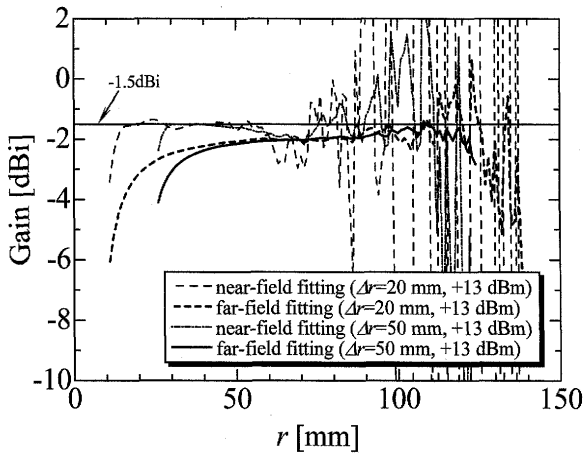

Fig. 10 Estimated gain of offset-fed dipole antenna by curve fitting for measured S_{21} based on extended Friis transmission formula in near-field region.

defined as effective wavelength in the liquid [4]. However, the far-field gain at $r = 100$ mm might be valid because the data used are satisfied by the above far-field condition. The level drops by about 17 dB for $|S_{21}|_{\mathrm{dB}}$ as the observation is moved from $r = 70$ mm to 100 mm, as seen from Fig. 7. In practice, the level of the measured $|S_{21}|$ at $r = 100$ mm is very low, almost equal to the noise floor level in the measurement system. This would be a serious problem to be solved when implementing our proposed calibration.

4.3 Near-Field Fitting for Measured Data

The measured S parameters can be applied to the regression analysis for the near-field fitting. The conditions for the experiment are the same as those described in Sect. 4.1. Figure 9 shows the measured $|S_{21}|$ and corresponding near-field fitting curve as a function of r. The estimated gain deviates from the measured data for $r \approx 0$ mm. This is because the contribution of the extremely near-field field with a distance dependency of $1/r^3$ is larger than the contribution of the Fresnel field with a distance dependency of $1/r^2$.

Figure 10 shows the near-field and far-field gains for $\Delta r = 20$ mm and 50 mm. In the same manner as was used to fit the simulated data, the near-field gain converges with the far-field gain even if the curve fitting is carried out with the data measured in the near-field region. As shown in Fig. 10, the near-field gain seems to be constant until $r = 60$ mm except for the initial rise, and the fluctuation is observed in the data for $r \geq 60$ mm. The near-field fitting fails to estimate the gain for $r \geq 60$ mm because the contribution of the far-field region is stronger than that of the near-field, so the asymptotic expansion of (17) is not well-behaved. The far-field gain suffers from the influence of its slow convergence, so the true gain cannot be obtained by estimating the far-field gain. Thus, the problem of measurement completely in the far-field region being impossible due to the large attenuation in the liquid is overcome by the near-field fitting in the near-field region. From the results of the near-field fitting, the permittivity and conductivity of the liquid are estimated to be 38.8 and 1.85 S/m, and the near-field gain is estimated to be −1.73 dBi.

5. Conclusion

The SAR probe calibration method above 3 GHz proposed in this paper can be implemented by calibrating the gain of reference antenna in tissue-equivalent liquid and relating the output voltage of the probe to the value of the electromagnetic fields or SAR. To implement this calibration, it is necessary to overcome the difficulties in measuring very low signal levels during far-field measurements that are caused by the excessive attenuation in the liquid. As one solution, we propose a method of estimating the gain of the reference antenna in the liquid after fitting the measured data to the curve based on the extended Friis transmitting formula in the near-field region of the antenna in the conducting medium. We applied the proposed method to both simulated and measured data and demonstrated its effectiveness at 2.45 GHz. Also, the enhancement of the dynamic range is useful in obtaining more accurate gain of the antenna in the liquid. In the future, we will calibrate the antenna gain in the liquid above 3 GHz and estimate its uncertainty.

References

[1] T. Akagawa, N. Ishii, K. Sato, L. Hamada, and S. Watanabe, "A gain measurement in the liquid based on Friis transmission formula in the near-field region," Proc. 2006 Int. Sym. Antennas Propagat., FC2-5, Singapore, Nov. 2006.

[2] IEC International Standard 62209-1, "Human exposure to radio frequency fields from hand-held and body-mounted wireless communication devices — Human models, instrumentation, and procedures — Part 1: Procedure to determine the specific absorption rate (SAR) for hand-held devices used in close proximity to the ear (frequency range of 300 MHz to 3 GHz)," 2005.

[3] K. Fukunaga, S. Watanabe, and Y. Yamanaka, "Dielectric properties of tissue-equivalent liquids and their effects on specific absorption rate," IEEE Trans. Electromagn. Compat., vol.46, no.1, pp.126–129, 2003.

[4] N. Ishii, K. Sato, L. Hamada, T. Iwasaki, and S. Watanabe, "Simulation of SAR-probe calibration using antennas in the liquid," Abst. Bioelectromagnetics 2005 (CD-ROM), 10-6, pp.99–101, Dublin,

Ireland, June 2005.
[5] N. Ishii, K. Sato, L. Hamada, and S. Watanabe, "Proposal of accurate SAR-probe calibration using reference antennas in the liquid at higher frequency," Proc. 28th General Assembly of the International Union of Radio Science (CD-ROM), A11.7, New Delhi, India, Oct. 2005.
[6] N. Ishii, K. Sato, L. Hamada, T. Iwasaki, and S. Watanabe, "A gain measurement of antennas in the tissue equivalent liquid for the SAR probe calibration," Abst. Bioelectromagnetics 2006 (CD-ROM), PB-8, pp.233–237, Cancun, Mexico, 2006.
[7] R.K. Moore, "Effect of a surrounding conducting medium on antenna analysis," IEEE Trans. Antennas Propag., vol.AP-11, no.3, pp.159–169, 1963.
[8] L.A. Ames, J.T. de Bettencourt, J.W. Frazier, and A.S. Orange, "Radio communications via rock strata," IEEE Trans. Commun. Syst., vol.CS-11, no.2, pp.159–169, 1963.
[9] C. Person, L.N. Ahlonsou, and C. Grangeat, "New test bench for the characterization of SAR measurement probes used in tissue equivalent liquid," Abst. Bioelectromagnetics 2000, P-116, pp.205–206, Munich, Germany, June 2000.
[10] C.A. Balanis, Antenna Theory Analysis and Design, 3rd ed., pp.1029–1030, John Wiley & Sons, New York, 2005.
[11] N. Ishii, Y. Yonemura, and M. Miyakawa, "Simultaneous measurement of antenna gain and solution dielectric properties," IEICE Trans. Commun., vol.E88-B, no.6, pp.2268–2274, June 2005.
[12] C.H. Wilcox, "An expansion theorem for electromagnetic fields," Commun. on Pure and Applied Math., vol.9, pp.115–134, 1954.
[13] M.K. Hu, "Near-zone power transmission formulas," 1958 IRE Nat'l Conv. Rec., vol.6, Pt. 8, pp.128–135, 1958.
[14] B.Y. Kinber and V.B. Tseytlin, "Measurement error of the directive gain and of the radiation pattern of antennas at short range," Radio Eng. Electron. Phys., pp.1304–1314, 1960.
[15] J.R. Pace, "Asymptotic formulas for coupling between two antennas in the Fresnel region," IEEE Trans. Antennas Propag., vol.AP-17, no.3, pp.285–291, 1969.
[16] R.E. Collin, "Radiation from simple sources," Chapter 2 in Antenna Theory part 1, ed. R.E. Collin and F.J. Zucker, p.40, McGraw-Hill, New York, 1969,
[17] J.A. Kong, Electromagnetic Wave Theory, p.509, EMW Publishing, Cambridge, MA, 2000.
[18] J.H. Richmond, "Computer program for thin-wire structure in a homogeneous conducting medium," Nat. Tech. Inform. Service, Rep. NASA CR-2399, 1975.

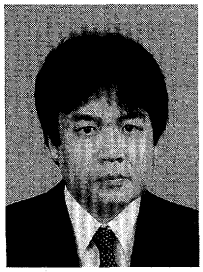

Nozomu Ishii received the B.S., M.S., and Ph.D. degrees from Hokkaido University, Sapporo, Japan, in 1989, 1991, and 1996, respectively. In 1991, he joined the faculty of Engineering at Hokkaido University. Since 1998, he has been with the faculty of Engineering at Niigata University, Japan, where he is currently an Associate Professor of the Department of the Biocybernetics. His current interests are in the area of small antenna, planar antenna, millimeter antenna, antenna analysis, antenna measurement, and electromagnetic compatibility. He is a member of the IEEE.

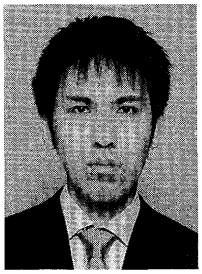

Takuhei Akagawa received B.S. and M.S. degrees in Niigata University in 2005 and 2007, respectively. He is currently an engineer with TOYO Corporation, Tokyo, Japan. When he was a graduate student of Niigata University, he engaged in the development of the system for calibrating SAR probes.

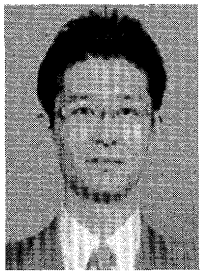

Ken-ichi Sato received the B.E. and M.E. degrees from Tamagawa University, Tokyo, Japan in 1993 and 1995, respectively. He joined NTT Advanced Technology Corporation, Tokyo, Japan in 1995. Since 1999, he is working in the field of the electromagnetic compatibility (EMC) problems including biomedical EMC issues, particularly in the Specific Absorption Radio (SAR) measurement.

Lira Hamada received the Ph.D. degree from Chiba University, Chiba, Japan, in 2000. From 2000 to 2005, she was with the Department of Electronics Engineering, University of Electro-Communications, Chofu, Tokyo, Japan. Since 2005, she has been with the National Institute of Information and Communications Technology (NICT), Koganei, Tokyo, Japan. She is a responsible researcher for the measurement and calibration technique for the SAR evaluation system. Dr. Hamada is a member of the IEE of Japan, the IEEE, and the Bioelectromagnetics Society.

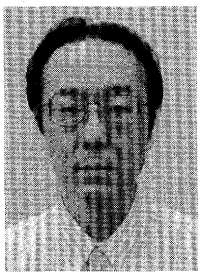

Soichi Watanabe received the B.E., M.E., and D.E., degrees in electrical engineering from Tokyo Metropolitan University, Tokyo, Japan, in 1991, 1993, and 1996, respectively. He is currently with the National Institute of Information and Communications Technology (NICT), Tokyo Japan. His main interest is research on biomedical electromagnetic compatibility. Dr. Watanabe is a member of the Institute of Electrical Engineers (IEE), Japan, the IEEE, and the Bioelectromagnetics Society. He was the recipient of several awards, including the 1996 International Scientific Radio Union (URSI) Young Scientist Award and 1997 Best Paper Award presented by the IEICE.